Hindawi Publishing Corporation
Journal of Nanomaterials
Volume 2013, Article ID 362175, 7 pages
http://dx.doi.org/10.1155/2013/362175

Research Article

Effect of Polymers (PEG and PVP) on Sol-Gel Synthesis of Microsized Zinc Oxide

Thilagavathi Thirugnanam

T. Agaram, 4/66 South Street, Tittakudi TK, Cuddalore District, Pennadam, Tamil Nadu 606105, India

Correspondence should be addressed to Thilagavathi Thirugnanam; tt.thilagavathi@yahoo.com

Received 11 December 2012; Revised 27 February 2013; Accepted 9 April 2013

Academic Editor: Alan K. T. Lau

Fibers irregular and seed-like microcrystalline ZnO were synthesized by using a cost-effective and low temperature aqueous sol-gel method. Various polymers, namely, polyethylene glycol 6000 (PEG 6000) and polyvinyl pyrrolidone (PVP), were used as structure directing agents. The samples were characterized by X-ray diffraction (XRD), Fourier transform infrared spectroscopy (FTIR), and scanning electron microscopy (SEM). The X-ray diffraction pattern revealed the formation of phase-pure ZnO micropowders. It is observed that the polymers play an important role in modifying the surface morphology and the size of the crystallites. A compact granular morphology is observed for the ZnO samples without polymer. The samples exhibit microparticles of size 100 nm for PVP and for PEG-mediated growth, whereas microporous corrugated morphology is observed for added PEG-mediated micropowder. FTIR study is used to confirm the structural modifications occurring in the polymers.

1. Introduction

Technology to control crystallization is a crucial requirement for the synthesis, purification, and application of materials in various industrial fields. In particular, ZnO (zinc oxide) is one of the most valuable materials in the study of crystal control because of its electronic and optical properties which are strongly influenced by the various morphologies, crystal sizes, dimensions, and aspect ratios. So far, much effort has been made in the synthesis of one-dimensional (1D) zinc oxide with various morphologies. It has been recognized as one of the materials with wide applicable possibilities in microelectronics, gas and piezoelectric sensors, emitters, transparent electrodes in solar cells, and in catalysis microtechnology [1–7].

Recently, extensive progress has been made on the research front of ZnO-based micromaterials motivated by both basic sciences and potential advanced technologies [8–21]. It also has interesting chemical, acoustic, optical, and electrical properties [22]. Various methods have been developed for the synthesis of ZnO microparticles, such as chemical vapor deposition onto Si substrate [23], electrodeposition [24], and vapor-liquid-solid (VLS) process on a substrate and hydrothermal or solvothermal treatment [25–27]. A recent work reports on the use of zinc acetate in water; however, this synthesis comprises a multistep process longer than a week. It is known that size of the microparticles can be controlled easily through the use of polymers in the system. Many polymers are known to have long hydrocarbon chain structures with hydrophobic ends. It is believed that this structure are critical in manipulating particle sizes.

The rate of particle aggregation is a major factor that controls the morphology and crystallinity of the final product. By adjusting the amount of PEG and PVP we can modify the size and morphology of the product. Reducing the amount of surfactant results in improving the crystallinity. It has been reported that PEG and PVP with uniform and ordered chain structure is easily absorbed at the surface of metal oxide colloid. When the surface of the colloid adsorbs PEG and PVP, the colloidal activities will greatly decrease and the growth rate of the colloids in some certain facet will be confined. Therefore, the addition of PEG and PVP in the reaction system will modify the kinetics of the growing process, which is attributed to the fact that the addition of PEG and PVP can elevate the crystallinity of samples and change the product morphology. In this present

work, the aim is to prepare low-cost advanced materials for photovoltaic energy production. We report a simple one-step, solid-state reaction in presence of PEG 6000 and PVP as size controlling agent for the preparation of ZnO microparticles. The process is carried out at room temperature. This method employed in the present study is polymer-assisted technique. The polymer-assisted method is used for the production of high surface area microparticles as well as for preventing microparticle agglomeration.

2. Experimental

2.1. Materials. Polyethylene glycol (PEG 6000), polyvinylpyrrolidone (PVP), zinc nitrate hexahydrate $Zn(NO_3)_2{\cdot}6H_2O$, and ammonium hydroxide ($NH_3{\cdot}H_2O$) were purchased from Aldrich. Solvent was spectroscopic grade and is being used without any further purification.

2.2. Preparation of ZnO with Polymer Additive. The suspension was prepared by sol-gel process with polyethylene glycol (PEG) and polyvinylpyrrolidone (PVP) as both the catalyst and the polymer. 1 g zinc nitrate hexa hydrate $Zn(NO_3)_2{\cdot}6H_2O$ and 0.3 g PEG (6000) and PVP with high purity were dissolved in 150 mL distilled water to form a transparent solution. With vigorous constant stirring, the 1.25 mL ammonium hydroxide $NH_3{\cdot}H_2O$ was added dropwise to the previous solution at room temperature. The resulting mixture was refluxed at 100°C for several hours and left to cool down naturally. Precipitates were collected and washed first with deionized water and then ethanol several times, respectively.

2.3. Materials Characterization. The phase structure of as-synthesized ZnO was performed using X-ray diffraction (Philips PW1370) with Cukα (λ = 1.54056), operating at 35 kV, and a scanning rate of 0.02%. The chemical structure of the prepared particles was performed by using a Fourier transform infrared (FTIR). Raman spectrometer (Nicolet Avatar impact 330 series) was used for measuring the ultraviolet absorption spectra in the region of 400–4000 cm^{-1} frequency range. The samples were characterized with a scanning electron microscope (SEM, JSM-5610 LV).

3. Result and Discussion

The XRD pattern of the pure ZnO products is shown in Figure 1(a). All the diffraction peaks are in good agreement with the JCPDS file for ZnO (JCPDS 36–1451, a = 3.249 Å), which can be indexed to the hexagonal wurtzite structure of ZnO. The strong and sharp diffraction peaks indicate that the ZnO microparticles are well crystallized [28–31]. The crystal size of the ZnO microparticles was calculated from FWHM (Table 1).

Figure 1(b) shows the X-ray diffraction pattern of the micro-ZnO with polymer additive. All the samples are polycrystalline with reflections along (002, 103, 200, 104, and 203) planes corresponding to hexagonal wurtzite zinc oxide. The XRD patterns for the products with and without

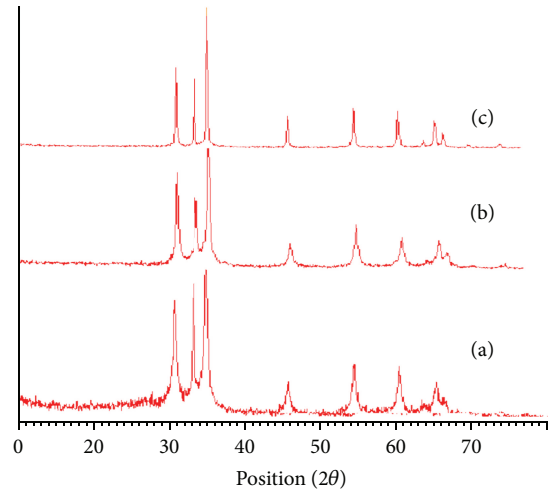

Figure 1: Powder X-ray diffraction (XRD) patterns of (a) pure Zno, (b) ZnO PEG, and (c) ZnO PVP.

polymers showed absolutely no difference. This revealed that the polymer did not affect the orientation of the samples. But it shows the high purity of the as-synthesized products. The XRD patterns indicate that well-crystallized hexagonal ZnO were obtained under present hydrothermal conditions [32].

The crystallite size of microcrystalline ZnO powders is calculated using the Scherrer formula $D = 0.9\lambda/\beta \cos\theta$, where D is crystallite size, λ is the wavelength of the X-rays, β is the full width at a half maximum intensity of the peaks, and θ is the diffraction angle, giving the value ranges for 10.73–19.75 nm for PEG 6000 in Table 1. The formation of ZnO, complex ion $Zn(NH_3)_4$, or $Zn(OH)_4^{2-}$ forms first by mixing $Zn(NO_3)_2$ and ammonia. With the presence of a water-soluble linear polymer (PEG 6000), zinc oxide crystal forms heterogeneous nucleus at the interface between substrate and solution by the dehydration of $Zn(OH)_4^{2-}$ or $Zn(NH_3)_4^{2+}$. Finally, after hydrothermal treatment the formation of ZnO tubes arrays complexes. In this work, the zinc amino complex $(Zn)NH_3)_4^{2+}$ formed and was controlled by the content of Zn^{2+} and NH^{3+}; PEG could promote the formation of crystalline ZnO nuclei. On the other hand, PEG could also be considered to influence the growth process of the ZnO. It was believed that the PEG has a great influence on ZnO microspheres. PEG is considered to be the adequate material. The reaction was not solid-state reaction but a liquid-state reaction, because the $Zn(NO_3)_2{\cdot}6H_2O$ had crystallization water which can be given off gradually during the reaction [33, 34].

The role of PVP in controlling the size and shape of microcrystalline ZnO powders which are calcined at 100°C for 3 hours. Figure 1(c) gives the XRD patterns with good crystallinity with the addition of PVP. The diffraction pattern and interplane spacing can be well matched to the standard diffraction pattern of wurtzite ZnO, demonstrating the formation of wurtzite ZnO microcrystals [35]. PVP plays two important roles in this system. First the PVP could promote the reaction of Zn^{2+} ions with NaOH to form $Zn(OH)_2$ by

Table 1: Particle size estimated from the diffraction spectrum of pure ZnO and ZnO + PEG and ZnO + PVP by using FWHM.

Pos. [°2Th.]	FWHM [°2Th.]	d-spacing [Å]	Particle size
ZnO			
20.6070	0.1624	4.30666	49.75
21.1017	0.3767	4.20680	21.46
31.7168	0.2223	2.81892	37.17
32.2752	0.2204	2.77141	37.55
36.2111	0.3289	2.47869	25.43
37.8471	0.1952	2.37522	43.05
39.4328	0.2219	2.28328	38.05
40.2274	0.2581	2.23999	30.82
46.2716	0.3002	1.96049	28.79
47.5163	0.3934	1.91199	22.08
51.9470	0.3629	1.75885	24.37
61.5732	0.3442	1.50496	26.88
ZnO + PEG			
31.7435	0.4185	2.81660	19.75
34.4296	0.7752	2.60276	10.73
36.2304	0.4763	2.47741	17.56
56.5610	0.6064	1.62583	14.88
62.8281	0.7628	1.47788	12.21
67.9014	0.6068	1.37928	15.79
76.8612	0.8850	1.23929	11.47
ZnO + PVP			
31.7805	0.2263	2.81341	36.52
36.2706	0.2261	2.47476	36.99
47.5571	0.2218	1.91045	39.16
56.6020	0.2782	1.62475	32.45
62.8752	0.2457	1.47689	37.92
66.4005	0.3162	1.40677	30.04
67.9614	0.3031	1.37821	31.63
69.0855	0.2729	1.35850	35.36
76.9490	0.2839	1.23809	35.77
31.7805	0.2263	2.81341	36.52

generating the OH^- groups in the solution. This phenomenon promoted reactions and grain growth. The PVP secondly acts as a stabilizer or capping agent higher than PEG.

Figure 2(a) shows the schematic of a capped ZnO microparticle; when PEG was added before synthesis, the increase in total particle size suggested the capping of microparticle with polymers. However, in the case of PEG addition after synthesis, the capping of microparticle with polymers did not happen as shown in Figure 2(b), since no change in both ZnO and total particle size was observed. In the case of PEG addition, the reason for the discrepancy before and after synthesis could be related to the polymer molecules being adsorbed to the ZnO microparticles. If the polymer molecules existed in the solution during the synthesis of ZnO microparticles, the chance of electrostatic adsorption to ZnO microparticles increased. Therefore, PEG molecules probably capped ZnO microparticles only when PEG was added to the solution before the synthesis of ZnO microparticle.

In the case of PVP addition before synthesis, the total particle size increased drastically, although ZnO particle size was almost the same. This change suggested the aggregation of PVP-capped ZnO microparticles, as shown in Figure 2(c). In the case of PVP addition after synthesis, particle size increased normally, although ZnO particle size was almost the same. This change suggested that ZnO microparticle was capped with polymers as shown in Figure 2(d). The discrepancy in the capping behavior between PEG and PVP could be attributed to the difference in adhesion strength. Because PVP has been widely known as a capping reagent for microparticles, adhesion of PVP was stronger than that of PEG. During the synthesis of ZnO microparticle, pH value of the solution was 6 at the beginning of synthesis and it was approximately 8 at the end of synthesis because of dropping sodium hydroxide.

ZnO microparticles were positively charged at the beginning of ZnO synthesis because pH value was less than a point of zero charge of ZnO. In the case of "before synthesis," polymer was added to the solution in this condition. On the other hand, ZnO microparticles were almost not charged at the end of ZnO synthesis because pH value was nearly equal to a point of zero charge of ZnO. In the case of "after synthesis," polymer was added to the solution in this condition. Although both PEG and PVP are nonionic surfactants, they would be partially charged. In particular oxygen in PVP would be charged more strongly than oxygen in PEG because of positively charged nitrogen in PVP. Therefore, PVP would electrostatically adhere to the surface of ZnO microparticle more strongly than PEG, especially in the case of "before synthesis." In the case of PVP, the result that the total particle size of the "before synthesis" was larger than "after synthesis" was obtained, which was the same as PEG.

FTIR spectrum is an effective method to reveal the composition of products. Figure 3(a) is a typical FTIR spectrum of pure ZnO, in which the peaks at 3402 cm^{-1} are assigned to the O–H stretching vibration. Symmetric C=O stretching of zinc acetate dehydrate at 1542 cm^{-1} and C–H out-of-plane bending group at 899–866 cm^{-1} are observed. O–H bending of the hydroxyl group at 559 cm^{-1} and stretching of ZnO at 420 cm^{-1}.

The FTIR spectra of the ZnO with PEG (Figure 3(b)) palletized with KBr were recorded over 4000–400 cm^{-1}. The spectra consist of seven vibrational bands. The bands at 3400–3600 cm^{-1} correspond to the O–H mode of vibration, that is, due to the hydroxyl group. The stretching mode of vibration corresponding to C=C is obtained at 1624 cm^{-1} and due to the alkyl group is obtained in the range of 2847–2926 cm^{-1}. The vibration due to the carboxyl group is obtained in the range of 1383–1399 cm^{-1}. The band at 464 cm^{-1} is due to zinc oxide and assigned to the stretching of ZnO–Zn.

The FTIR spectrum of synthesized ZnO powder (Figure 3(c)) presented main absorption bands due to O–H stretching of the hydroxyl group at 3402 cm^{-1}, asymmetric and symmetric C=C. A peak at 1654 cm^{-1} is assigned to the stretching vibration of the C=O in the PVP. The other

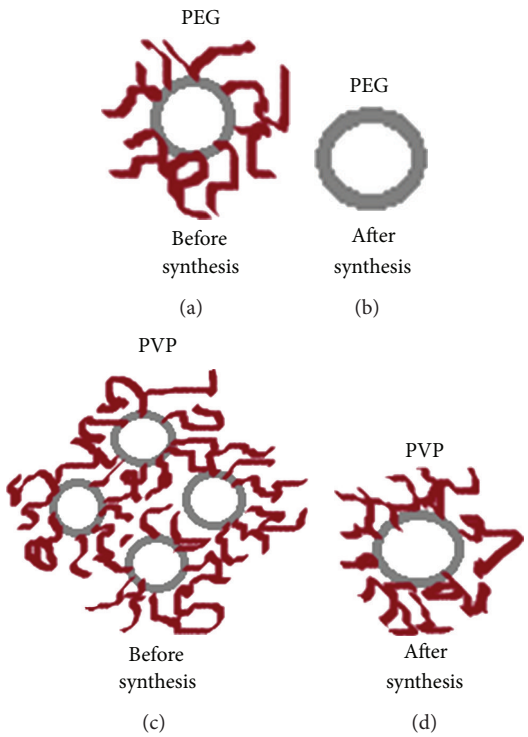

Figure 2: Schematic of ZnO microparticles capped by polymer molecules: (a) PEG was added to the ZnO solution before synthesis; (b) PEG was added to the ZnO solution after synthesis; (c) PVP was added to the ZnO solution before synthesis; (d) PVP was added to the ZnO solution after synthesis.

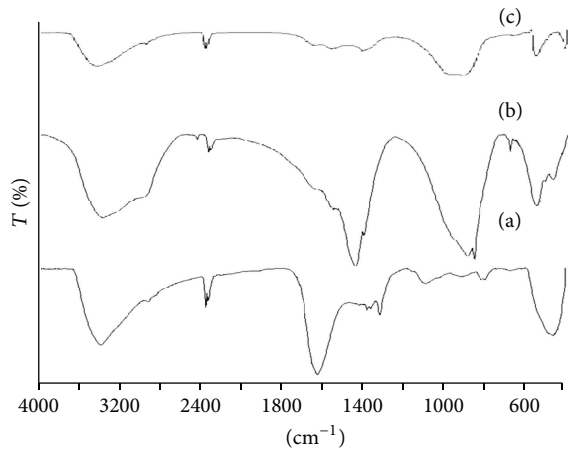

Figure 3: FTIR spectra of (a) pure ZnO (b) ZnO PEG, and (c) ZnO PVP.

important peaks at 1285 cm^{-1} and 1438 cm^{-1} are referring the C–N is stretching vibration and the attachment of CH_2 groups in the pyrrole ring of PVP. The O–H bending of the hydroxyl group at 569 cm^{-1} and Zn–O stretching of ZnO at 431 cm^{-1}. These data are similar to the results observed by Suwanboon [36].

Low-magnification SEM image (Figure 4) shows the overall morphology of the ZnO hollow spheres with and without polymer. ZnO consists of nearly uniform spheres with diameters ranging from 400 to 600 nm and the thickness of the shell is approximately 80 nm are shown in Figure 4(a). High-magnification SEM image shows that the outer surface of the hollow spheres is rough and stacked with small microparticles standing out of the surface. Furthermore, irregular sponge like structure could be observed on the surface of those spheres. Figures 4(b) and 4(c) display the SEM image of a cracked sphere with apparent cavity, demonstrating the hollow nature of the as-prepared ZnO spheres. It can be also found that the inner surface of the hollow sphere is also coarse and consists of small microparticles with an average diameter of about 40 nm. It is worth noting that the hollow sphere is built from a single shell of small microparticles without any substrate support. Figure 4(d) shows the uniformly arranged grains like ZnO conglomeration which is a porous micron sphere.

Figures 4(e) to 4(l) show the SEM image of zinc oxide with PEG and PVP as a synthetic polymer. It is found that the product is composed of well-defined crystals with irregular spherical-like structure on the substrate on a large scale are shown in Figure 4(e). Moreover, these microparticles are irregularly shaped on the whole, yet coexisting with minor amounts of well-defined hexagonal structures. Figures 4(f) and 4(g) show a large number of irregular particles with the size of 1 μm which complies well with that of the precursor in shape and it consists of major amount of irregular particles and minor amount of plate-like structures.

Particularly, these plates take on novel porous structures as highlighted in the inset of Figure 4(h). In the presence of PEG the morphology is completely different than that obtained from pure ZnO.

Figures 4(i), 4(j), 4(k), and 4(l) show the SEM image of zinc oxide with PVP. The PVP has a structure with a polyvinyl skeleton with polar groups as reported by Inamdar et al. [37]. The lone pair of nitrogen and oxygen in a polar group of one PVP unit may occupy the orbital of the metal ion. The Zn^{+2} can coordinate with PVP, which can take part in controlling the grain size and morphology of ZnO by reducing the reaction rate. The PVP can adsorb on different faces due to the formation of beads-like structure. It is supported that, in the presence of PVP, smaller grains (Figures 4(k) and 4(l)) are formed due to aggregation rate.

4. Conclusion

Microcrystalline ZnO powders have been synthesized in an aqueous solution by a simple method using PEG and PVP as precursors. These powders have been indexed as wurtzite or hexagonal structure with the smallest average crystallite size of about 10.73–19.75 nm for PEG and 30.04–39.16 nm for PVP. The addition of these polymers probably led to capping ZnO microparticles, which passivate surface defects. This phenomenon depends on the timing of the addition of the polymer to the ZnO solution. The experimental results of the PVP addition before the synthesis of ZnO microparticles indicated the aggregation of capped microparticles. The morphology of ZnO has altered from irregular spherical

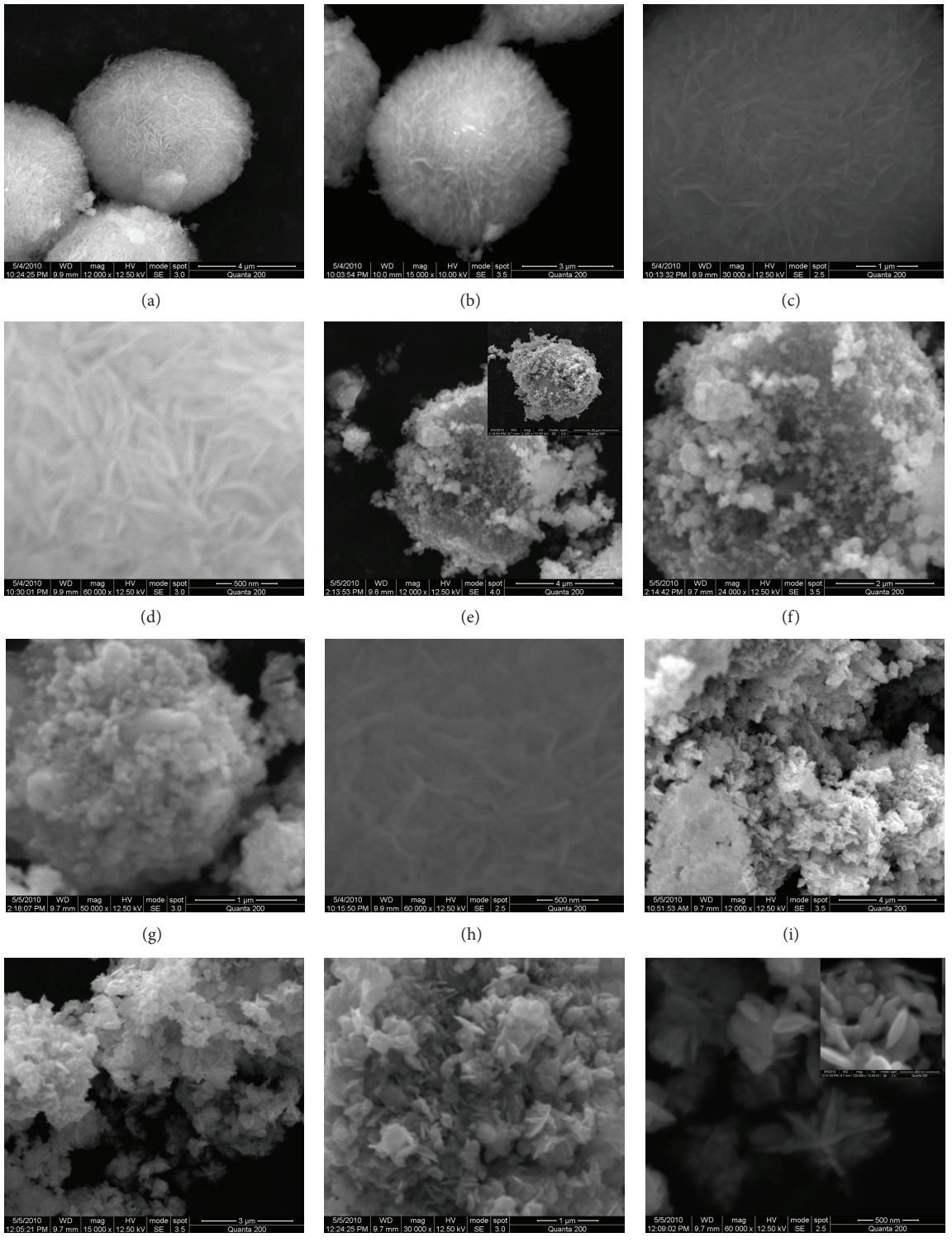

Figure 4: SEM images of as-prepared pure ZnO (a, b, c, and d), ZnO PEG (e, f, g, and h), and ZnO PVP (i, j, k, and l) with different magnification.

and beads-like structure when adding PEG and PVP into solution. Thus we conclude that PVP is found to be dominant in altering the morphologies of ZnO.

References

[1] J. H. Jang, J. H. Park, and S. G. Oh, "Effects of dodecyl sulfate anionic surfactants on the crystal growth of ZnO through hydrothermal process," *Journal of Ceramic Processing Research*, vol. 10, no. 6, pp. 783–790, 2009.

[2] S. Rani, P. Suri, P. K. Shishodia, and R. M. Mehra, "Synthesis of nanocrystalline ZnO powder via sol-gel route for dye-sensitized solar cells," *Solar Energy Materials and Solar Cells*, vol. 92, no. 12, pp. 1639–1645, 2008.

[3] S. S. Kim, J. H. Yum, D. Y. Kim, and Y. E. Sung, "Electrophoretically deposited TiO_2 photo-electrodes for use in flexible dye-sensitized solar cells," *Journal of Photochemistry and Photobiology A*, vol. 173, no. 1, pp. 1–6, 2005.

[4] X. F. Wang, O. Kitao, and E. Hosono, "TiO_2- and ZnO-based solar cells using a chlorophyll a derivative sensitizer for light-harvesting and energy conversion," *Journal of Photochemistry and Photobiology A*, vol. 210, pp. 145–152, 2010.

[5] A. Al-Hajry, A. Umar, Y. B. Hahn, and D. H. Kim, "Growth, properties and dye-sensitized solar cells-applications of ZnO nanorods grown by low-temperature solution process," *Superlattices and Microstructures*, vol. 45, no. 6, pp. 529–534, 2009.

[6] D. M. Fernandesa, R. Silva, A. A. W. Hechenleitner, E. Radovanovic, M. A. C. Melo, and E. A. G. Pineda, "Synthesis and characterization of ZnO, CuO and a mixed Zn and Cu oxide," *Materials Chemistry and Physics*, vol. 115, pp. 110–115, 2009.

[7] O. M. Lemine, M. A. Louly, and A. M. Al-Ahmari, "Planetary milling parameters optimization for the production of ZnO nanocrystalline," *International Journal of Physical Sciences*, vol. 5, no. 17, pp. 2721–2729, 2010.

[8] F. Sheng, C. Xu, J. Guo, G. Zhu, and Q. Chen, "Structural, electronic and Infrared spectral properties of ZnO hexagonal nanodisks with different saturate conditions," *Science of Advanced Materials*, vol. 3, pp. 709–718, 2011.

[9] Z. Zhou, Y. Zhao, and Z. Cai, "Low-temperature growth of ZnO nanorods on PET fabrics with two-step hydrothermal method," *Applied Surface Science*, vol. 256, no. 14, pp. 4724–4728, 2010.

[10] J. Wu and D. Xue, "Progress of science and technology of ZnO as advanced material," *Science of Advanced Materials*, vol. 3, no. 2, pp. 127–149, 2011.

[11] Y. Liu, A. Liu, W. Liu, Z. Hu, and Y. Sang, "Characterization of optoelectronic properties of the ZnO nanorod array using surface photovoltage technique," *Applied Surface Science*, vol. 257, no. 4, pp. 1263–1266, 2010.

[12] L. S. Roselin and R. Selvin, "Photocatalytic degradation of reactive orange 16 dye in a ZnO coated thin film flow photoreactor," *Science of Advanced Materials*, vol. 3, no. 2, pp. 251–258, 2011.

[13] M. Gusatti, C. E. M. Campos, J. A. Rosario, D. A. R. Souza, N. C. Kuhnen, and H. G. Riella, "The rapid preparation of ZnO nanorods via low-temperature solochemical method," *Journal of Nanoscience and Nanotechnology*, vol. 11, pp. 5187–5192, 2011.

[14] P. Zhang, G. D. Zhou, H. B. Gong et al., "Pressure-induced growth evolution of different ZnO nanostructures by a pulsed Laser Ablation method," *Science of Advanced Materials*, vol. 4, pp. 455–462, 2012.

[15] J. Yang, J. Lang, C. Li et al., "Effects of substrate on morphologies and photoluminescence properties of ZnO nanorods," *Applied Surface Science*, vol. 255, no. 5, pp. 2500–2503, 2008.

[16] P. K. Samanta and P. R. Chaudhuri, "Growth and optical properties of chemically grown ZnO nanobelts," *Science of Advanced Materials*, vol. 3, no. 1, pp. 107–112, 2011.

[17] P. K. Samanta, "Characteristics of benzene assited grown ZnO nanosheets," *Science of Advanced Materials*, vol. 4, pp. 219–226, 2012.

[18] W. J. Liu, X. Q. Meng, Y. Zheng, and W. Xia, "Synthesis and photoluminescence properties of ZnO nanorods and nanotubes," *Applied Surface Science*, vol. 257, no. 3, pp. 677–679, 2010.

[19] T. M. Milao, V. R. de Mendonca, V. D. Araujo et al., "Microwave hydrothermal synthesis and photocatalytic performance of ZnO and M:ZnO nanostructures (M = V, Fe, Co)," *Science of Advanced Materials*, vol. 4, pp. 54–60, 2012.

[20] G. N. Dar, A. Umar, S. A. Zaidi et al., "Fabrication o high-sensitive non-enzymatic glucose biosensor based on ZnO nanorods," *Science of Advanced Materials*, vol. 3, pp. 901–906, 2011.

[21] A. Umar, M. S. Akhtar, A. Al-Hajry, M. S. Chauhan, and S. Chauhan, "Growth, properties and dye-sensitized solar cells (DSSCs) applications of ZnO Nanocones and small nanorods," *Science of Advanced Materials*, vol. 3, pp. 695–701, 2011.

[22] W. Lee, M. C. Jeong, and J. M. Myoung, "Catalyst-free growth of ZnO nanowires by metal-organic chemical vapour deposition (MOCVD) and thermal evaporation," *Acta Materialia*, vol. 52, no. 13, pp. 3949–3957, 2004.

[23] Y. Leprince-Wang, A. Yacoubi-Ouslim, S. Tusseau-Nenez, and G. Y. Wang, "Study of electrodeposited thin films and microwires ZnO," in *Proceedings of the 4th International Conference on Inorganic Materials (ICIM '04)*, pp. 19–21, Antwerp, Belgium, September 2004.

[24] Z. Fan and J. G. Lu, "Zinc oxide microstructures: synthesis and properties," *Applied Physics Letters*, vol. 86, no. 123, p. 510, 2005.

[25] L. S. Panchakarla, M. A. Shah, A. Govindaraj, and C. N. R. Rao, "A simple method to prepare ZnO and $Al(OH)_3$ nanorods by the reaction of the metals with liquid water," *Journal of Solid State Chemistry*, vol. 180, no. 11, pp. 3106–3110, 2007.

[26] T. M. Hammad, J. K. Salem, and R. G. Harrison, "Binding agent effect on the structural and optical properties of ZnO microparticles," *Reviews on Advanced Materials Science*, vol. 22, pp. 74–80, 2009.

[27] H. Xu, H. Wang, Y. Zhang et al., "Hydrothermal synthesis of zinc oxide powders with controllable morphology," *Ceramics International*, vol. 30, no. 1, pp. 93–97, 2004.

[28] J. Xie, P. Li, Y. Li, Y. Wang, and Y. Wei, "Solvent-induced growth of ZnO particles at low temperature," *Materials Letters*, vol. 62, no. 17-18, pp. 2814–2816, 2008.

[29] J. Xie, P. Li, Y. Li, Y. Wang, and Y. Wei, "Morphology control of ZnO particles via aqueous solution route at low temperature," *Materials Chemistry and Physics*, vol. 114, no. 2-3, pp. 943–947, 2009.

[30] H. J. Zhai, W. H. Wu, F. Lu, H. S. Wang, and C. Wang, "Effects of ammonia and cetyltrimethylammonium bromide (CTAB) on morphologies of ZnO nano- and micromaterials under solvothermal process," *Materials Chemistry and Physics*, vol. 112, no. 3, pp. 1024–1028, 2008.

[31] D. Yiamsawas, K. Boonpavanitchakul, and W. Kangwansupamonkon, "Preparation of ZnO microstructures by solvothermal method," *Journal of Microscopy Society of Thailand*, vol. 13, pp. 75–78, 2009.

[32] Z. Xu, J. Y. Hwang, B. Li, X. Huang, and H. Wang, "The characterization of various ZnO nanostructures using field-emission SEM," *Journal of Management*, vol. 26, no. 4, pp. 29–32, 2008.

[33] S. Erten-Ela, S. Cogal, and S. Icli, "Conventional and microwave-assisted synthesis of ZnO nanorods and effects of PEG400 as a surfactant on the morphology," *Inorganica Chimica Acta*, vol. 362, no. 6, pp. 1855–1858, 2009.

[34] X. M. Liu and Y. C. Zhou, "Seed-mediated synthesis of uniform ZnO nanorods in the presence of polyethylene glycol," *Journal of Crystal Growth*, vol. 270, no. 3-4, pp. 527–534, 2007.

[35] P. Gu, X. Wang, T. Li, H. Meng, H. Yu, and Z. Fan, "Synthesis, characterization and photoluminescence of ZnO spindles by polyvinylpyrrolidone-assisted low-temperature wet-chemistry process," *Journal of Crystal Growth*, vol. 338, pp. 162–165, 2012.

[36] S. Suwanboon, "Structural and optical properties of nanocrystalline ZnO powder from sol-gel method," *ScienceAsia*, vol. 34, no. 1, pp. 31–34, 2008.

[37] A. I. Inamdar, S. H. Mujawar, V. Ganesan, and P. S. Patil, "Surfactant-mediated growth of nanostructured zinc oxide thin films via electrodeposition and their photoelectrochemical performance," *Nanotechnology*, vol. 19, no. 32, Article ID 325706, 7 pages, 2008.